Polym. Bull. (2012) 68:1921–1934
DOI 10.1007/s00289-011-0679-5

ORIGINAL PAPER

Synthesis and liquid crystalline behavior of phosphorus-containing aliphatic–aromatic copoly(ester-imide)s

Ionela-Daniela Carja · Diana Serbezeanu · Tăchiţă Vlad-Bubulac · Corneliu Hamciuc · Maria Brumă

Received: 29 August 2011 / Revised: 14 November 2011 / Accepted: 27 November 2011 /
Published online: 4 December 2011
© Springer-Verlag 2011

Abstract A series of phosphorus-containing copoly(ester-imide)s was prepared by polycondensation reaction of 2-(6-oxido-6*H*-dibenz<c,e><1,2>oxaphosphorin-6-yl)-1,4-naphthalene diol, **1**, or of various mixtures of **1** and 1,12-dodecanediol, **3**, with an aromatic diacid chloride containing preformed imide rings, **2**, namely 4-chloroformyl-*N*-(*p*-chloroformylphenyl)-phthalimide. The polymers exhibited thermotropic liquid crystalline behavior, as was observed by means of polarized light microscopy, differential scanning calorimetry, and X-ray investigations. The copoly(ester-imide)s showed good thermal stability having the temperature of 5% weight loss above 365–408 °C and char yield at 700 °C in the range 8.8–48%.

Keywords Poly(ester-imide)s · Phosphorus-containing polymers · Thermal stability · Thermotropic liquid crystalline behavior

Introduction

Aromatic polyimides are well-known polymers which possess high thermal stability, good mechanical properties and chemical resistance, and low dielectric constant, thus being versatile engineering polymers. Due to their unique properties these polymers have a wide range of potential applications in several modern technologies. They are very suitable for electro-insulating materials and protective layers and coating formulations for aircraft, automotive, and aerospace applications, as well as matrix resins for high performance light weight composites [1–3]. However, because of their chain rigidity and strong interchain interaction, most polyimides are insoluble in common organic solvents and intractable in their

I.-D. Carja · D. Serbezeanu (✉) · T. Vlad-Bubulac · C. Hamciuc · M. Brumă
"Petru Poni" Institute of Macromolecular Chemistry, Aleea Gr. Ghica Vodă 41A,
700487 Iasi, Romania
e-mail: diana.serbezeanu@icmpp.ro

imidized forms [4, 5]. Significant efforts in the area of aromatic polyimides have been made to improve the solubility and processability through the incorporation of flexible linkages into the monomers or by the introduction of supplemental heterocyclic units in the main chain, or bulky substituents along the polymer backbone [6–8]. It has been demonstrated that the incorporation of phosphorus atom into the polymers increases the solubility, thermal stability, and fire-retardant properties [9–17].

Phosphorus-containing polymers have been the focus of considerable research interest not only for the flame retardancy but also on a more fundamental level because they exhibit a range of unusual liquid crystalline behaviors. Liquid crystalline polymers are particularly attractive due to their potential applications in optical switching, optical data storage, and optical display [18–20].

As novel flame retardants, 9,10-dihydro-9-oxa-10-phosphaphenanthrene-10-oxide (**DOPO**) and its derivative 2-(6-oxido-6*H*-dibenz<c,e><1,2>oxaphosphorin-6-yl)-1,4-naphthalene diol have been extensively studied [21–23]. The research study, however, is mainly focused on the characterization of flame retardancy of polymers based on such compounds. Few researchers took into consideration the application of thermotropic liquid crystalline polymer (TLCP) in the field of improving flame retardancy of ignitable polymers [24]. Introduction of phosphorus-containing bulky groups into the macromolecular chain of TLCP can enhance the flame retardancy of the polymer, and it can also decrease the melt temperature of TLCP due to its branching effect [25, 26].

Previously, liquid crystalline poly(ester-imide)s were synthesized by Lenz starting from 4-chloroformyl-*N*-(*p*-chloroformylphenyl)-phthalimide and various aliphatic diols, in which the number of methylene spacers varies from 4 to 12, by solution polycondensation in refluxing 1,2,4-trichlorobenzene [27]. The family of such polymers abbreviated as PEIM(*n*), where *n* represents the number of methylene units in the structure, has the same chemical structure as those synthesized by Kricheldorf's group which found that PEIMs with even number of CH_2 form a crystalline state with a layered supermolecular order, a so-called crystalline smectic state [28–31].

To further investigate the relationship between the aliphatic/aromatic ratio, and the liquid crystalline phase structure and thermo-oxidative stability of polymers, we have synthesized a series of thermotropic liquid crystalline aromatic-aliphatic copoly(ester-imide)s by the reaction of, various mixtures of 2-(6-oxido-6*H*-dibenz<c,e><1,2>oxaphosphorin-6-yl)-1,4-naphthalene diol, **1**, and 1,12-dodecanediol, **3**, with 4-chloroformyl-*N*-(*p*-chloroformylphenyl)-phthalimide, **2**.

Experimental

Materials

DOPO was purchased from Chemos GmbH, Germany. Naphthoquinone (NQ), *p*-aminobenzoic acid, trimellitic anhydride, thionyl chloride, and 1,12-dodecanediol

were provided from Aldrich and used as received. All other reagents were used as received from commercial sources or were purified by standard methods.

Measurements

Melting points of the monomers and intermediates were measured on a Melt-Temp II (Laboratory Devices). The inherent viscosities of the polymers, η_{inh}, were measured using an Ubbelohde viscosimeter, at 20 °C by using 0.5 g/dL solutions in *N*-methylpyrrolidone. Fourier transform infrared (FT-IR) spectroscopy was performed on a Bruker Vertex 70 at frequencies ranging from 400 to 4,000 cm^{-1}. Samples were mixed with KBr and pressed into pellets. ^1H NMR (400 MHz) spectra were obtained on a Bruker Avance DRX 400 spectrometer. The polymer samples were dissolved in $CHCl_3$/trifluoroacetic acid (9/1, v/v) and then measured at room temperature. The differential scanning calorimetry (DSC) analysis was carried out using a Perkin-Elmer Pyris Diamond instrument using nitrogen as a carrier gas at a flow rate of 10 mL/min. The samples were first heated from room temperature to 200 °C using a heating rate of 10 °C/min. The melting temperatures and the liquid crystalline phase transition temperatures of polymers were taken as maximum of endothermic peaks. Polarized light microscopy (PLM) was carried out with an Olympus BH-2 polarized light microscope fitted with a THMS 600/HSF9I hot stage, at a magnification of 200× or 400×. The mesomorphic transition temperature and disappearance of birefringence, that is, the crystal-to-nematic (T_m) and nematic-to-isotropic (T_i) transition, were noted. The wide-angle X-ray diffraction (WAXD) experiments at room temperature were performed on a D8 Advance Bruker AXS diffractometer using a Cu-Kα source with an emission current of 36 mA and a voltage of 30 kV. Scans were collected over the $2\theta = 2$–40 range using a step size of 0.01° and a count time of 0.5 s/step. FT-IR spectroscopy in attenuated total internal reflection (ATR) configuration has been applied to the study of mesomorphic behavior of polymer **4d**, in the temperature range of 25–140 °C. The temperature-dependent FT-IR–ATR spectra were recorded in heating runs, on a Vertex 70 (Bruker, Germany) spectrometer equipped with a Golden Gate ATR accessory (Specac Ltd.) and a temperature controller. The single reflection IRE was diamond, with an incidence angle of 45°. The measurements were performed in the 4,000–600 cm^{-1} spectral range, at a heating rate of 5 °C/min, with 64 scans, at 2 cm^{-1} resolution. Thermogravimetric analysis (TGA) was performed on 15 mg samples under air atmosphere at a heating rate of 10 °C/min using a Mettler Toledo model TGA/SDTA 851 instrument.

Synthesis of the monomers

4-Chloroformyl-*N*-(*p*-chloroformylphenyl)-phthalimide, **2**, was obtained by treating with excess thionyl chloride, at reflux temperature, the corresponding dicarboxylic acid resulting from the condensation of trimellitic anhydride with *p*-aminobenzoic acid; mp: 194–195 °C. FT-IR (KBr, cm^{-1}): 1780 (C=O of imide ring and COCl), 1720 (C=O of imide ring), 1600 (aromatic), 1390 (C–N), 1100 and 720 (imide ring).

^{1}H NMR (DMSO-d_6, ppm): $\delta = 8.38$ (1H, d), 8.29 (1H, s), 8.12 (1H, s,), 8.05 (2H, s), 7.65 (2H, d) [32].

2-(6-Oxido-6*H*-dibenz<c,e><1,2>oxaphosphorin-6-yl)-1,4-naphthalene diol, **1**, was synthesized from **DOPO** and NQ [33]. It was recrystallized from ethoxyethanol; mp (DSC): 279–280 °C. FT-IR (KBr, cm^{-1}): 3430 (–OH), 1582 (P–Ar), 1190 (P=O), 1165 and 925 (P–O–Ar). ^{1}H NMR (DMSO-d_6, ppm): $\delta = 7.9$ (2H, m), 7.8 (1H, m), 7.7 (1H, m), 7.5 (4H, m), 7.4 (1H, m), 7.3 (1H, m), 7.2 (1H, t), 7.1 (1H, t), 6.6 (1H, d).

Synthesis of the polymers

The synthetic route of the polymers **4** is presented in Scheme 1. The poly(ester-imide) **4a** was obtained by solution polycondensation reaction of diacid chloride **2** with aromatic naphthalene diol **1**; this polymer was previously reported and here it was used for comparison with the new polymers [11]. The copoly(ester-imide)s **4b–4d** have been prepared by solution polycondensation reaction of diacid chloride **2** with a mixture of naphthalene diol **1** and **3**, taken in various ratios, according to Scheme 1. The experimental details are described below using polymer **4c** as example: 0.374 g (0.001 mol) of aromatic naphthalene diol **1**, 0.202 g (0.001 mol) of aliphatic diol **3**, 0.696 g (0.002 mol) of diacid chloride **2**, and 7 mL of *o*-dichlorobenzene were introduced in a 100-mL flask equipped with magnetic stirrer and nitrogen inlet and outlet. The reaction mixture was refluxed for 20 h and then it was cooled to room temperature. The product was filtered off, washed with methanol, and dried at 100 °C for 5 h. The polymer was purified by reprecipitation in methanol from chloroform/trifluoroacetic acid (9/1, v/v) and dried at 80 °C for 8 h under vacuum. Yield: 89%. The same procedure was used to synthesize the copoly(ester-imide)s **4b** and **4d**.

Results and discussion

Synthesis, chemical structure confirmation, and general characterization of the polymers **4**

The aromatic–aliphatic polymers **4b–4d** were synthesized from 2-(6-oxido-6*H*-dibenz<c,e><1,2>oxaphosphorin-6-yl)-1,4-naphthalene diol, **1**, 4-chloroformyl-*N*-(*p*-chloroformylphenyl)-phthalimide, **2**, and aliphatic diol **3**, by heating the reaction mixture for 20 h at reflux temperature (180 °C) using *o*-dichlorobenzene as reaction medium. The reaction system became temporarily homogeneous, and then the polymers precipitated during the polycondensation process. The inherent viscosities of the polymers, measured in *N*-methylpyrrolidone, were in the range of 0.11–0.26 dL/g (Table 1), suggesting moderate molecular weights for this type of PEIs.

The structure of the polymers was confirmed by FT-IR and ^{1}H NMR spectroscopies. Figure 1 shows the FT-IR spectrum of polymer **4d**, as example. As can be seen, the most important absorption bands are associated with aromatic

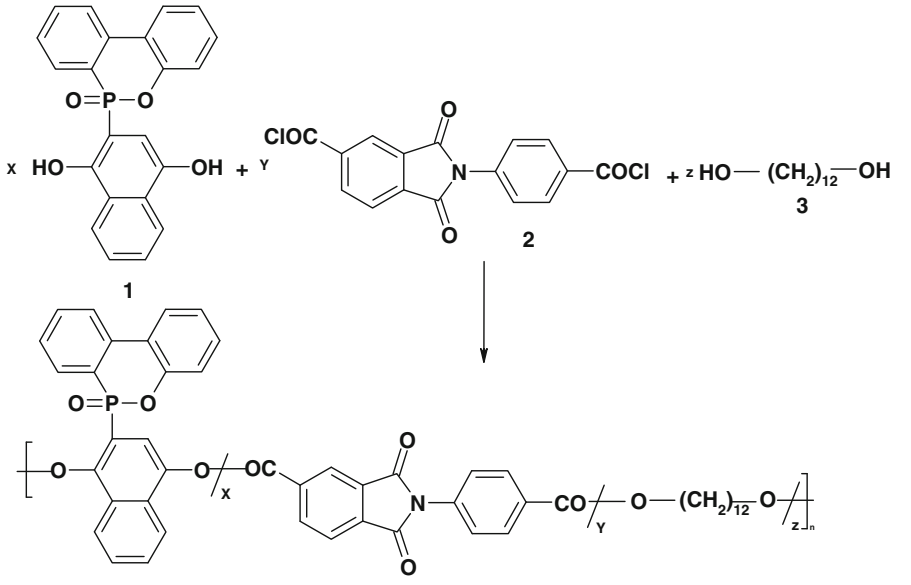

	x	y	z
4a	1	1	0
4b	0.75	1	0.25
4c	0.5	1	0.5
4d	0.25	1	0.75

Scheme 1 Synthesis of the polymers **4**

Table 1 Inherent viscosity and solubility of polymers **4**

Polymer	η_{inh}	NMP	DMAc	DMF	THF	$CHCl_3$	$CHCl_3$/TFA	Acetone
4a	0.26	+	+	+	−	±	+	−
4b	0.22	+	+	+	−	+	+	−
4c	0.16	+	+	+	−	+	+	−
4d	0.11	+	+	+	−	+	+	−

NMP N-methylpyrrolidone, *DMAc N,N*-dimethylacetamide, *DMF N,N*-dimethylformamide, *THF* tetrahydrofuran, *TFA* trifluoroacetic acid, + soluble, ± partially soluble, − insoluble

C–H (3068 cm^{-1}, stretching vibration), aliphatic C–H (2920 and 2851 cm^{-1} asymmetric and symmetric stretching vibrations), C=O groups of imide rings and ester linkages (1783 and 1724 cm^{-1}, asymmetric and symmetric stretching

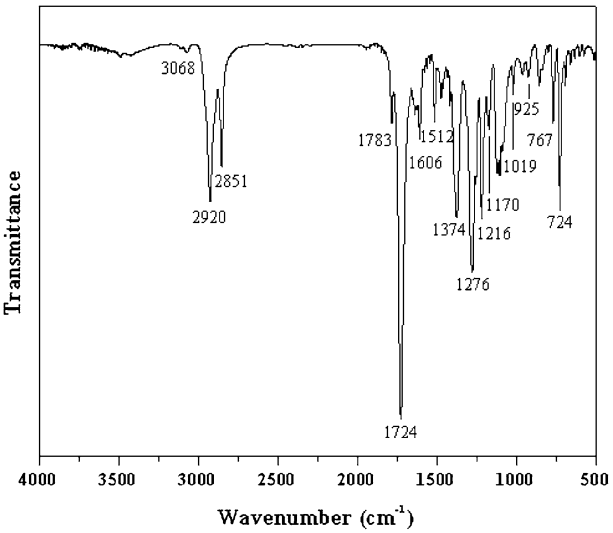

Fig. 1 FT-IR spectrum of polymer **4d**

vibrations, ester C–O–C (1276 and 1019 cm^{-1}, asymmetric and symmetric stretching vibrations), P–O–Ar (925 and 1170 cm^{-1}, stretching vibrations), P–Ar (1471 cm^{-1}), P=O (1216 cm^{-1}), aromatic C–H (767 cm^{-1}, deformation vibration caused by the 1,2-disubstituted aromatic **DOPO** rings [34, 35]. Characteristic absorptions of aromatic C=C bands were found at 1606 and 1512 cm^{-1}.

The ^{1}H NMR spectrum of the polymer **4b** (recorded in $CDCl_3/CF_3COOH$ = 9/1, v/v) is presented in Fig. 2 with the assignments for all protons. The protons H_{14}, H_{15}, and H_{16} closed to imide ring appeared at higher ppm in the ^{1}H NMR spectrum (8.58–8.35 ppm). The protons of **DOPONQ** unit appeared in the range of 8.19–7.25 ppm. The polymer showed characteristic peaks of the aliphatic protons, one singlet which corresponds to the methylene groups located in the α-position of the ester linkages (O–C$\underline{H}_2$, $4H_{19}$, $\delta \cong 4.35$ ppm) and one singlet which corresponds to the methylene groups located in the β-position of the ester linkages, respectively (O–CH_2–C$\underline{H}_2$, $4H_{20}$, $\delta \cong 1.8$ ppm). The peak characterizing the other methylene groups of the structural unit (C$\underline{H}_2$, $16H_{21}$) appeared at $\delta \cong 1.45$–1.25 ppm. From the ^{1}H NMR spectra of the copolymers it was found that the composition of the polymer is similar with the composition of the reactants used in synthesis.

The solubility of the polymers **4** was tested in various solvents, by using 15 mg polymer/mL solvent, at room temperature, and the results are presented in Table 1. All the polymers were easily soluble in polar aprotic solvents like *N*-methylpyrrolidone, *N*,*N*-dimethylformamide, or *N*,*N*-dimethylacetamide. The poly(ester-imide) **4a** exhibited limited solubility in chloroform, while the copoly(ester-imide)s **4b**–**4d** were easily soluble. The higher solubility of these polymers can be explained by the presence of dodecane segments which increase the flexibility of the macromolecular chains and the free volume of the polymer thus increasing the solubility. All the polymers **4** were easily soluble in a mixture of chloroform/trifluoroacetic acid 9/1 (v/v).

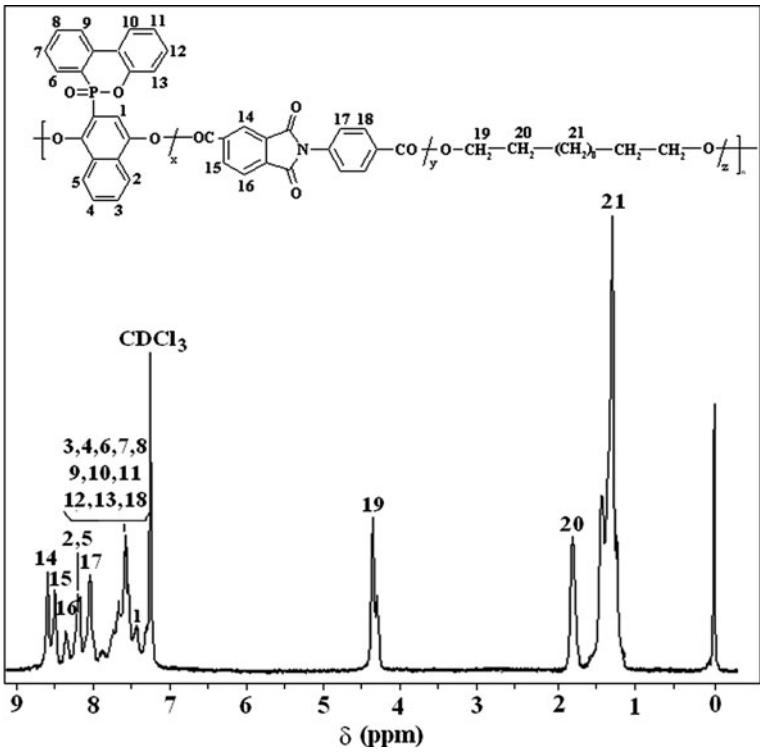

Fig. 2 ^{1}H NMR spectrum of polymer **4b**

Liquid crystalline properties

Polarized light microscopy

The morphological textures of the polymers were studied as a function of temperature in a hot-stage polarized light microscope. Photomicrographs of different textures are shown in Fig. 3. The data of the mesomorphic transition temperature are given in Table 2. A suitable amount of sample for each polymer was charged between two clean glass plates. The samples were heated up to clearing point, which is considered as the liquid crystalline to isotropic state transition.

The transition temperatures from crystal to liquid crystalline melt were in the range of 108–329 °C and depended on the aliphatic content. Thus, the polymer **4a** without methylene units had the highest value for the transition K → LC (329 °C). The LC → I transition temperatures for the polymers **4** were in the range of 139–389 °C. Isotropization temperature (T_i) greatly depends on the content of phosphorus-containing monomer **1**. The transition temperatures of the polymers **4** obtained by PLM were compared with those measured by differential scanning calorimetry. These two methods gave comparable results as seen in Table 2. The observed differences could be explained by the variation of the heating–cooling rate, amounts of the sample used for the

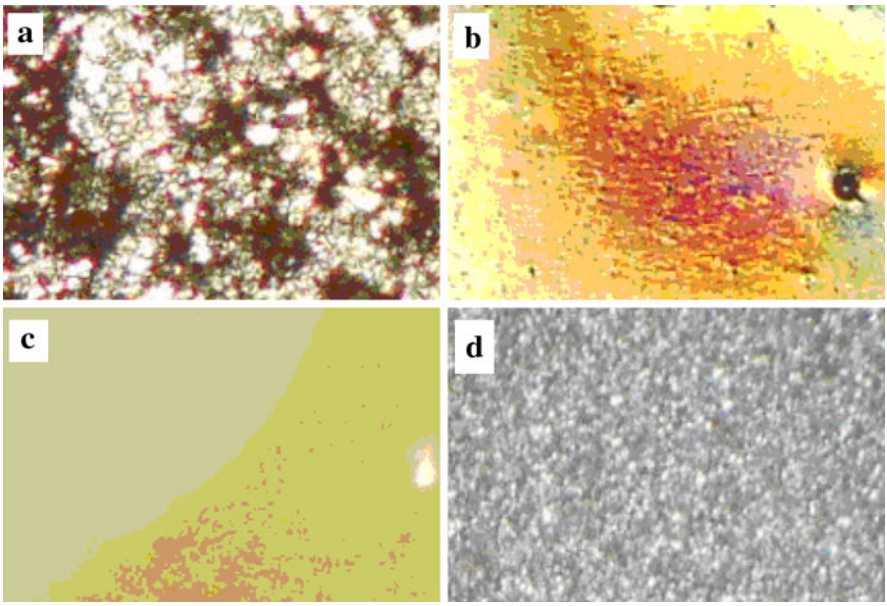

Fig. 3 Optical micrographs of polymers **4**: **a** polymer **4b** during heating cycle at 195 °C; **b** polymer **4d** heating cycle up to 121 °C; **c** polymer **4b** heating cycle up to 273 °C; and **d** polymer **4b** cooling cycle at 135 °C showing fine droplets appearance from the isotropic state

Table 2 Phase transition temperatures of synthesized polymers **4**

Polymer	PLM[a]		DSC[b]	
	K → LC	LC → I	T_g	Thermal transitions
4a	329	389	195	–
4b	139	273	–	K_1 96 K_2 137 LC (-) I
4c	108	143	–	K_1 61 K_2 83 LC 143 I
4d	112	139	–	K_1 58 K_2 84 LC 138 I

T_g glass transition temperature, K_1, K_2 solids, *LC* liquid crystalline phase, *I* isotropic state, (-) peak temperature not observed by DSC

[a] Phase transition temperature taken from PLM observation, first heating cycle at a heating rate of 10 °C/min

[b] Peak temperatures from DSC were taken as the phase transition temperature

measurements, or the presence of the different atmosphere (nitrogen, in the case of DSC, and air, in the case of the PLM investigation).

Upon heating all as-synthesized polymers **4** formed fine textures, difficult to ascribe to a smectic or nematic phase. The polymer **4a** formed nematic phase according to the observation of its optical texture on a cross-polarizing microscope. When the LC polymer melt sheared on glass plates, they exhibited fine LC textures (Fig. 3a, b). The isotropic phase for polymer **4b** can be observed in Fig. 3c. On cooling from the isotropic state, the sample **4b** exhibited fine droplets (Fig. 3d).

Thermal transitions behavior

The thermal properties and the phase transition temperatures of the synthesized polymers were determined by DSC and are summarized in Table 2. Figure 4 shows typical DSC heating curves of the polymers **4c** and **4d**, at a heating rate of 10 °C/min. The polymer **4a** showed T_g at 195 °C. The as-synthesized polymer **4b** exhibited a broad tiny endotherm centered at 97 °C and a broad endotherm centered at 137 °C, which corresponded to a K to LC and no peak temperature for the nematic-to-isotropic transition. The DSC traces of the polymers **4c** and **4d** show melting endotherms centered at 61 °C/83 °C and 58 °C/84 °C, respectively, while the liquid crystalline to isotropic state transitions appeared at 143 and 138 °C, respectively. The lower melting temperature (T_m) values for these polymers compared to related poly(ester-imide)s without aliphatic segments have been attributed to the presence of aliphatic diol unit leading to more disordered arrangements.

X-ray diffraction

The mesophases of the polymers were also characterized through X-ray diffraction measurements. Representative XRD curve for **4d** at room temperature is shown in Fig. 5. The sample **4d** showed sharp and strong peaks at low angle ($2\theta \sim 3.28°$ and 6.24°, respectively), and strong sharp peaks in wide angle ($2\theta \sim 16.52°$ and 22.73°). Other studied polymers showed relatively broad reflections at wide angles (associated with the lateral packing) and only one weak sharp reflection at small angles (associated with weak smectic layers), which evidenced the inability to identify smectic organizations under DSC and PLM observations [36]. The percent crystallinity of the polymers was determined by bisecting the experimental plot into the crystalline domain and amorphous domain by curve fitting. The areas under the crystalline and amorphous domains were determined computationally and the percentage crystallinity was calculated. The polymers **4c** and **4d** exhibited the percentage crystallinity equal to 38.73 and 50.26%, respectively. The percentage crystallinity decreased upon increasing the content of aromatic diol, which

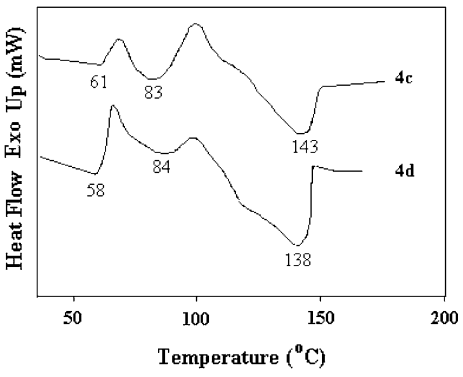

Fig. 4 DSC thermograms of polymers **4c** and **4d**

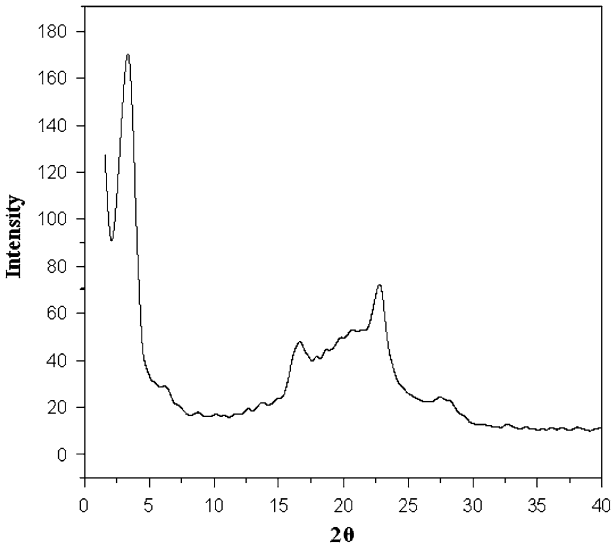

Fig. 5 XRD pattern of the polymer **4d** at room temperature

illustrates repressed crystallization capacities and deregulated molecular packing as a result of the presence of bulky lateral **DOPO** groups.

FT-IR–ATR analysis

The FT-IR–ATR analysis was used to investigate the changes in the peak position, bandwidth or area of the bands and splitting of some fundamentals, modifications which are related to the mesomorphic behavior and order–disorder transition. It was considered that the most sensitive ways of molecular packing are both scissoring (1469 cm^{-1}) and rocking modes (724 cm^{-1}) of CH_2 vibrations [37–39]. The thermally induced changes on the C–H stretching modes provide information about conformational mobility of the alkyl chains. As can be seen in Fig. 6, in the region of CH aliphatic stretching vibrations, the spectrum remained essentially unchanged during the K → LC phase transition and only an increase of the overall intensity could be noted. In the LC phase, the splitting of the CH_2 absorption bands was still preserved. When the temperature increased to 110 °C, several absorbance peaks were noted. In Fig. 6a, it can be seen that the peaks at 2920 and 2851 cm^{-1}, which were attributed to asymmetrical and symmetrical stretching of the methylene group, respectively, decreased with increasing temperature. The phase transition can also be monitored by using the stretching vibrations of the phosphorous groups. Figure 6b presents the temperature-dependent FT-IR–ATR spectra in the 1600–600 cm^{-1} spectral region. When the temperature increased to 110 °C the absorbance band of P=O groups was observed in the spectrum at 1216 cm^{-1}. The peak position was slowly shifted to the red with increasing temperature, from 1216 to 1215 cm^{-1}, as the long-range order of crystalline phase was reduced to a short-range one. During

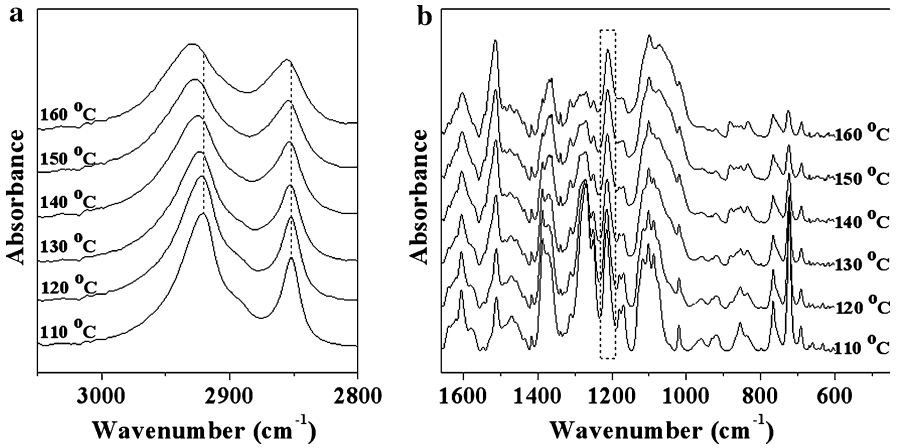

Fig. 6 FT-IR–ATR spectra of polymer **4d** at various temperatures **a** in the 3000–2800 cm^{-1} region and **b** in the 1600–600 cm^{-1} region

LC → I phase transition, the frequency decreased (1212 cm^{-1}) and the absorption band was broadened at small wavenumbers. This might be due to a rearrangement of the **DOPO** bulky groups.

Thermal stability

The thermo-oxidative stability of the polymers was evaluated by TGA in air at a heating rate of 10 °C/min. The thermogravimetric (TG) curve and the differential weight loss (DTG) curve for polymer **4c** are presented in Fig. 7. The most important TGA data (the initial decomposition temperature, temperature of DTG peaks, and the yields of char residue at 700 °C) are illustrated in Table 3. The polymers did not show significant weight loss below 365 °C. They began to decompose in the range of 365–408 °C, and showed 10% weight loss in the range of 380–423 °C.

As can be seen from differential thermogravimetric curves (DTG), the weight loss process in air exhibited two maxima. The first maximum of decomposition (T_{max1}) was in the range of 400–447 °C and it was due to the decomposition of ester units and aliphatic moieties which were more sensitive to degradation. The second maximum of decomposition (T_{max2}) was in the range of 555–595 °C and it was attributed to the degradation of aromatic polymer chain itself (Table 3). The char yields at 700 °C were in the range of 8.8–48% (Table 3). The high percentage of char yield (48%) in case of polymer **4a** may be attributed to the formation of a higher amount of phosphoric acid which acts as a fire-retardant agent in the condensed phase mechanism [25]. A decrease of char yield at 700 °C was observed by introduction of a higher content of aliphatic diol; thus, the polymer **4d** having the highest content of aliphatic segment showed the lowest char yield, 8.8%.

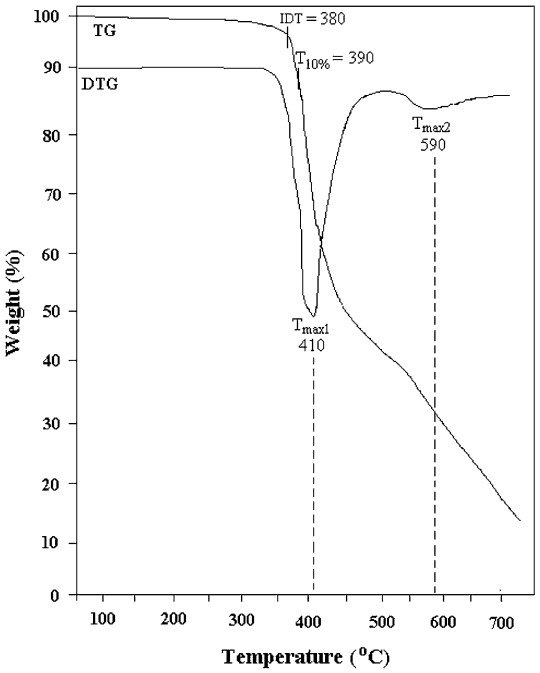

Fig. 7 TG and DTG curves of the polymer **4c**

Table 3 Thermal properties of the polymers **4**

Polymer	IDT[a] (°C)	T_{10}^{b} (°C)	T_{max1}^{c} (°C)	T_{max2}^{d} (°C)	Char yield at 700 °C (%)
4a	408	423	447	593	48.0
4b	365	380	400	595	24.0
4c	380	390	410	590	18.8
4d	370	390	420	555	8.8

[a] Initial decomposition temperature: the temperature of 5% weight loss

[b] Temperature of 10% weight loss

[c] First maximum polymer decomposition temperature

[d] Second maximum polymer decomposition temperature

Conclusions

A series of aliphatic–aromatic poly(ester-imide)s containing phosphorous bulky groups has been prepared by polycondensation reaction of aromatic imide–diacid chloride with a mixture of a phosphorous-containing diol with an aliphatic diol taken into various ratios. These polymers exhibited thermotropic liquid crystalline properties as evidenced by PLM, DSC, and X-ray diffraction measurements. Their transition temperatures decreased by increasing the content of aliphatic segment. These polymers showed high thermal stability with decomposition temperatures being above 365 °C as seen in TG analysis. The char yield at high temperature

(700 °C) increased from 8.8 to 24% by increasing the amount of phosphorus-containing monomer from 0.25 to 0.75 mol in 1 mol mixture of diols and it reached 48% when only phosphorous-containing diol was used in the reaction with diacid chloride.

Acknowledgments This study was supported by CNCSIS-UEFISCSU, project number PN II-RU 657/2010.

References

1. Mittal KL (1984) Polyimides, vol 1 and 2. Plenum Press, New York
2. Liu JG, Li XZ, He MH, Wang FS, Yang SY (2003) Fluorinated copolyimides for microelectronics applications. In: Mittal KL (ed) Polyimides and other high temperature polymers, vol 2. VSP BV, Utrecht, pp 447–458
3. Liaw DJ, Chang FC, Leung MK, Chou MY, Muellen K (2005) High glass transition and rigid-rod of novel organosoluble polyimides and polyamides based on bulky and noncoplanar naphthalene group without ether linkage. Macromolecules 38(9):4024–4029
4. Sroog CE (1991) Polyimides. Prog Polym Sci 16(4):561–694
5. Takekoshi T (1996) Synthesis of polyimides. In: Ghosh MK, Mittal KL (eds) Polyimides: fundamentals and applications. Marcel Dekker, New York, pp 7–46
6. Huang SJ, Hoyt AE (1995) The synthesis of soluble polyimides. Trends Polym Sci 3(8):262–271
7. Shang Y, Fan L, Yang S, Xie X (2006) Synthesis and characterization of novel fluorinated polyimides derived from 4-phenyl-2,6-bis[4-(4′-amino-2′-trifluoromethyl-phenoxy)phenyl]pyridine and dianhydrides. Eur Polym J 42(5):981–989
8. Wang L, Zhao Z, Li J, Chen C (2006) Synthesis and characterization of fluorinated polyimides for pervaporation of *n*-heptane/thiophene mixtures. Eur Polym J 42(6):1266–1272
9. Liu YL, Tsai SH (2002) Synthesis and properties of new organosoluble aromatic polyamides with cyclic bulky groups containing phosphorus. Polymer 43(21):5757–5762
10. Lu SY, Hamerton I (2002) Recent developments in the chemistry of halogen-free flame retardant polymers. Prog Polym Sci 27(8):1661–1712
11. Chang YL, Wang YZ, Ban DM, Yang B, Zhao GM (2004) Heat induced structure modifications in polymer-layered silicate nanocomposites. Macromol Mater Eng 289(4):703–714
12. Vlad-Bubulac T, Hamciuc C, Petreus O, Bruma M (2006) Synthesis and properties of new phosphorus-containing poly(ester-imide)s. Polym Adv Technol 17(9–10):647–652
13. Vlad-Bubulac T, Hamciuc C, Petreus O (2006) Synthesis and properties of some phosphorus-containing polyesters. High Perform Polym 18(3):255–264
14. Hamciuc C, Vlad-Bubulac T, Sava I, Petreus O (2006) New phosphorus-containing copolyesters. J Macromol Sci Part A 43(9):1355–1363
15. Levchik SV, Weil ED (2006) A review of recent progress in phosphorus-based flame retardants. J Fire Sci 24(5):345–364
16. Hamciuc C, Vlad-Bubulac T, Petreus O, Lisa G (2008) Synthesis and characterization of new aromatic polyesters and poly(ester-imide)s containing phosphorous cyclic bulky groups. Polym Bull 60(5):657–664
17. Sponton M, Ligadas G, Ronda JC, Galia M, Cadiz V (2009) Development of a DOPO-containing benzoxazine and its high-performance flame retardant copolybenzoxazines. Polym Degrad Stabil 94(10):1693–1699
18. Han M, Ichimua K (2001) In-plane and tilt reorientation of *p*-methoxyazobenzene side chains tethered to liquid crystalline polymethacrylates by irradiation with 365 nm light. Macromolecules 34(1):90–98
19. Natansohn A, Rochon P (2002) Photoinduced motions in azo-containing polymers. Chem Rev 102(11):4139–4175
20. Ikeda T (2003) Photomodulation of liquid crystal orientations for photonic applications. J Mater Chem 13(9):2037–2057
21. Qian L, Zhi J, Tong B, Shi J, Yang F, Dong Y (2009) Synthesis and characterization of main-chain liquid crystalline copolyesters containing phosphaphenanthrene side-groups. Polymer 50(20):4813–4820

22. Vlad-Bubulac T, Hamciuc C (2009) Aliphatic–aromatic copolyesters containing phosphorous cyclic bulky groups. Polymer 50(10):2220–2227
23. Serbezeanu D, Vlad-Bubulac T, Hamciuc C, Aflori M (2010) Structure and properties of phosphorous-containing thermotropic liquid-crystalline aliphatic–aromatic copolyesters. Macromol Chem Phys 211(13):1460–1471
24. Wang YZ, Chen XT, Tang XD, Du XD (2003) A new approach to simultaneous improvement of the flame retardancy, tensile strength and melt dripping of polyethylene terephthalate. J Mater Chem 13(6):1248–1249
25. Senthil S, Kannan P (2001) Ferrocene-based organophosphorus liquid-crystalline polymers: synthesis and characterization. J Polym Sci Part A 39(14):2396–2403
26. Senthil S, Kannan P (2004) Novel thermotropic liquid crystalline polyphosphonates. Polymer 45(11):3609–3614
27. Ricardo P, Zhang A, Gabori PA, Harris FW, Cheng SZD, Adduci J, Facinelli JV, Lenz RW (1992) Monotropic liquid crystal behavior in two poly(ester imides) with even and odd flexible spacers. Macromolecules 25(19):5060–5068
28. Kricheldorf HR, Jahnke P (1990) LC-poly(imide)s-4. Poly(ester imide)s derived from naphthalene-1,4,5,8-tetracarboxylic acid, ω-amino acids and α,ω-dihydroxyalkanes and their low molecular weight models. Eur Polym J 26(9):1009–1015
29. Kricheldorf HR, Domschke A, Schwarz G (1991) Liquid-crystalline polyimides. 3. Fully aromatic liquid-crystalline poly(ester imide)s derived from *N*-(4-carboxyphenyl)trimellitimide and substituted hydroquinones. Macromolecules 24(5):1011–1016
30. Kricheldorf HR, Schwarz G, de Abajo J, de la Campa JG (1991) LC-Polyimides: 5. Poly(ester-imide)s derived from *N*-(4-carboxyphenyl) trimellitimide and α,ω-dihydroxyalkanes. Polymer 32(5):942–949
31. Kricheldorf HR, Huner R (1992) LC-Polyimides. VII. Thermotropic poly(ester-imide)s derived from trimellitic acid with phosphonate or phosphate groups in the main chain. J Polym Sci Part A 30:337–341
32. Neamtu G, Bruma M (1982) Copolyimides new polybenzoxazinone-imides. Angew Macromol Chem 103:19–27
33. Sun YS, Wang CS (2001) Synthesis and luminescent characteristics of novel phosphorus containing light-emitting polymers. Polymer 42(3):1035–1045
34. Socrates G (2004) Infrared and Raman characteristics groups frequencies, tables and charts, 3rd edn. Wiley, Chichester
35. Thomas LC (1974) Interpretation of infrared spectra of organophosphorus compounds. Heyden, London
36. Meng FB, Cui Y, Chen HB, Zhang BY, Jia C (2009) Phase behaviors of comb-like liquid crystalline polysiloxanes containing fluorinated mesogenic units. Polymer 50(5):1187–1196
37. Casal HL, Mantsch H (1983) The thermotropic phase behavior of N-methylated dipalmitoylphosphatidylethanolamines. Biochim Biophys Acta 735:387–396
38. Androsch R, Kolesov I, Radusch HJ (2003) Temperature-resolved derivative FTIR. J Therm Anal Calorim 73(1):59–70
39. Cozan V, Avadanei M, Perju E, Timpu D (2009) FTIR investigation of phase transitions in an asymmetric azomethine liquid crystal. Phase Transit 82(8):607–619